IOPscience iopscience.iop.org

Home Search Collections Journals About Contact us My IOPscience

# Use of multiple acoustic reflections to enhance SAW UV photo-detector sensitivity

This content has been downloaded from IOPscience. Please scroll down to see the full text.

2017 Smart Mater. Struct. 26 035029

(http://iopscience.iop.org/0964-1726/26/3/035029)

View the table of contents for this issue, or go to the journal homepage for more

Download details:

IP Address: 195.208.255.154
This content was downloaded on 17/02/2017 at 10:56

Please note that terms and conditions apply.

You may also be interested in:

High performance dual-wave mode flexible surface acoustic wave resonators for UV light sensing
X L He, J Zhou, W B Wang et al.

Ultraviolet sensing based on nanostructured ZnO/Si surface acoustic wave devices
Y J Guo, C Zhao, X S Zhou et al.

Low-intensity ultraviolet detection using a surface acoustic-wave sensor with a Ag-doped ZnO nanoparticle film
Chen Fu, Ki Jung Lee, Keekeun Lee et al.

High-frequency acoustic charge transport in GaAs nanowires
S Büyükköse, A Hernández-Mínguez, B Vratzov et al.

Shadow mask assisted direct growth of ZnO nanowires as a sensing medium for surface acoustic wave devices using a thermal evaporation method
Ajay Achath Mohanan, R Parthiban and N Ramakrishnan

Study on the performance of ZnO nanomaterial-based surface acoustic wave ultraviolet detectors
Wenbo Peng, Yongning He, Xiaolong Zhao et al.

Growth of ZnO thin films on interdigital transducer/Corning 7059 glass substrates by two-step fabrication methods for surface acoustic wave applications
Mu-Shiang Wu, Wen-Ching Shih and Woo-Hu Tsai

Structural, optical and transport studies of nanocomposite SnOx thin films grown by DC sputter deposition and post-annealing
V V Siva Kumar and D Kanjilal

IOP Publishing Smart Materials and Structures
Smart Mater. Struct. **26** (2017) 035029 (6pp) https://doi.org/10.1088/1361-665X/26/3/035029

# Use of multiple acoustic reflections to enhance SAW UV photo-detector sensitivity

**G Y Karapetyan[1], V E Kaydashev[1], D A Zhilin[1], T A Minasyan[1], K G Abdulvakhidov[2] and E M Kaidashev[1]**

[1] Laboratory of Nanomaterials, Southern Federal University, Stachki 200/1, 344090 Rostov-on-Don, Russia
[2] Physics Faculty, Southern Federal University, Zorge 5, 344090 Rostov-on-Don, Russia

E-mail: kaydashev@gmail.com

Received 12 May 2016, revised 23 August 2016
Accepted for publication 13 September 2016
Published 13 February 2017


**Abstract**

A new approach to enhance the sensitivity of existing SAW UV-visible photo-detectors based on the monitoring of the multiple reflections of the acoustic waves in the Fourier transform of the frequency response ($S_{21}$) is demonstrated. By using this concept, it is possible to monitor the UV-visible light in a wide intensity range from very high to ultralow. We present a strategy to obtain an ultrafast SAW UV photo-detector with millisecond response by tuning the deposition conditions of the ZnO film and using the multiple-reflections concept.

Keywords: SAW, surface acoustic wave, UV detector, ZnO

(Some figures may appear in colour only in the online journal)

## 1. Introduction

Ultraviolet surface acoustic wave (UV SAW) photo-detectors allow us to use the benefits of resistive type photo-detectors to build more complicated SAW-based devices. Typically, a semiconductor layer is deposited onto a channel where SAW propagates, or a layer of the piezoelectric semiconductor itself is a SAW propagation channel [1–5]. An incident light with photon energy higher than a semiconductor band gap is absorbed with generating electron–hole pairs. An electric field of a SAW propagating on the surface of the acoustic channel penetrates the semiconductor and interacts with carriers generated by light. The acousto-electronic interaction results in (i) the increase of insertion loss for the propagating wave and (ii) a reduction in surface-wave velocity, which is observed as a phase shift and a SAW arrival delay [2, 5].

Attenuation, velocity/phase or frequency shift in SAW-based devices are nonlinear functions of an acoustic wavelength, incident light wavelength and intensity. The acoustic wavelength is defined by the geometry of the interdigital transducers (IDTs) and properties of the acoustic channel. Whereas the wavelength selectivity and sensitivity of the ZnO-based SAW photo-detector are defined by the properties of the semiconductor.

There are several approaches to enhance the sensitivity of a SAW photo-detector, namely by designing a device working at higher frequencies [5, 6], by the use of semiconductor nanowire arrays [7] and nanoparticles [8] and/or plasmon nanoparticles [9] to increase the light harvesting. Indeed, the performance of a SAW photo-detector is normally considerably enhanced at higher frequencies. In particular, it was shown that for the ZnO/ZnMgO/ZnO/a-$Al_2O_3$ UV photo-detector the insertion loss change in the Sezawa wave mode at 711.3 MHz is higher than the one for the Rayleigh wave mode at 545.9 MHz [5]. The high sensitivity observed as an extreme SAW oscillator frequency shift of 1017 kHz was obtained under illumination at 385 nm, 551 $\mu$W cm$^{-2}$ [6]. However, the number of oxygen vacancies and structural peculiarities of a light-sensitive ZnO layer has a major effect on the sensitivity and response/relaxation time of a photo-detector [8, 10]. For instance, the SAW oscillator presented by Kumar *et al* [11] was capable of detecting ultralow UV-light intensity of 450 nW cm$^{-2}$. However, the detector suffered from relatively slow photo-response (tens of seconds), caused by oxygen deficiency of the ZnO film. Moreover, the majority of the previously reported SAW photo-detectors suffered from inadmissibly slow photo responses and long recovery times of 2.4–30 s [7, 8, 10, 12–14] and only in rare studies were faster responses achieved [9].

 © 2017 IOP Publishing Ltd Printed in the UK

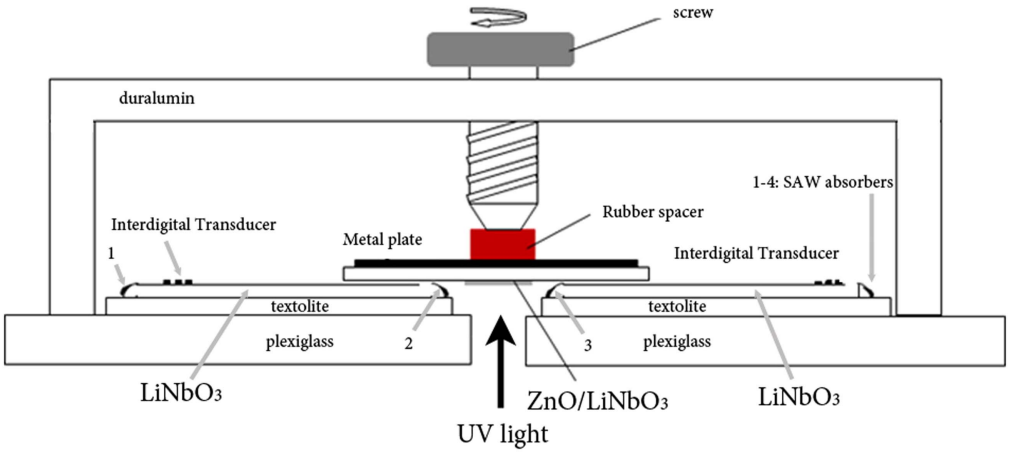


**Figure 1.** Experimental setup to study the properties of the SAW UV photo-detector.

In this paper, we report on a new approach to enhance the sensitivity of existing ZnO/$LiNbO_3$ SAW UV-visible photo-detectors. In contrast to previous approaches applied to SAW-based light detection, we use second, third and higher-order reflections of the acoustic wave to monitor low UV-light intensity. We also demonstrate that a ZnO layer prepared under different conditions may drastically modify the major characteristics of a photo-detector. We report on the strategy to build a SAW UV detector, in which both ultrafast photo-response and high sensitivity may be achieved.

## 2. Experimental details

ZnO films were deposited onto the central part of a (1 × 2) cm 128° YX $LiNbO_3$ substrate by pulsed laser deposition at an oxygen pressure of $2–5 \cdot 10^{-2}$ mbar and a temperature of 500 °C (Sample 1) and 550 °C (Sample 2), similar to the procedure reported elsewhere [15]. Laser ablation was done by focusing a KrF (248 nm) laser beam on a rotating ZnO ceramic target to give a fluence of 2 J $cm^{-2}$. The target to substrate distance was set to be 5 cm and a ∼250 nm thick film was deposited for 4000 laser pulses.

Q1 To avoid the SAW propagation losses inserted by the edges of the ZnO film, we do not use a mask during the deposition. A homogeneous deposition area of ∼1 × 1 cm is defined by laser-plume geometry. Our approach to excite and detect a SAW differs from those applied in previous studies, where IDTs are deposited onto the UV-sensitive film. We use two 128° YX $LiNbO_3$ substrates with one-directional IDTs on each piece to guide the SAW to the sample and detect the corresponding signal. The examined ZnO/128° YX $LiNbO_3$ sample is mounted on the top of these two substrates near their edges, as shown in figure 1.

The acoustic channels of the sample transmitter and receiver substrates are positioned on the same line to allow the SAW to propagate from one substrate to another. The SAW generated by the IDT on the first substrate passes to the ZnO/$LiNbO_3$ sample and then passes to the third substrate with the detecting IDT. The polished $LiNbO_3$ surfaces are tightly pressed to each other using a metal plate and rubber spacer, which guarantee a homogeneous press. Thus, a substrate break is avoided. IDTs have a central frequency of 120.7 MHz. The $LiNbO_3$ substrate edges are rounded and are covered by absorbers. SAW absorbers should not touch the examined sample so that it does not block the propagating wave. We deliberately separate the ZnO/ $LiNbO_3$ sample from the IDTs. This approach ensures that we do not deposit the IDTs onto the examined film, thus providing more flexibility for technological procedures, such as heat treatment and further growth of nanostructures onto the semiconductor film, without the risk of the metallic constructions being damaged. Note that a high-quality ZnO crystalline film needed as a high-quality detector is normally obtained at an elevated temperature of 450 °C–650 °C. The possible contamination of the ZnO film surface with chemicals or film degradation during the lithography step are also excluded in this way. The use of this approach is a forced arrangement and a good alternative to the lift-off procedure often used to overcome the technological difficulties [16].

## 3. Results and discussion

Figure 2 shows that an x-ray defraction (XRD) curve of the deposited ZnO film revealed peaks at 34.5°, 32.9°, 68.8°, corresponding to ZnO (002), $LiNbO_3$ (104) and (208) crystal orientations with ZnO (002)||$LiNbO_3$ (104) figure 2. The full width at half maximum (FWHM) for the ZnO (002) peak is 0.3°, showing the high crystalline quality of the film.

When the ZnO/$LiNbO_3$ structure is exposed to UV light, extra carriers are generated in the ZnO layer. The SAW velocity change ($\Delta v$) and wave intensity attenuation ($\Gamma$) induced by acousto-electric interaction are given by [16]

$$\frac{\Delta v}{v_0} = \frac{k_{ef}^2}{2}\frac{1}{1+\sigma^2/\sigma_m^2} \quad \Gamma = k_{ef}^2\left(\frac{\pi}{\lambda}\right)\frac{\sigma/\sigma_m}{1+\sigma^2/\sigma_m^2},$$

where $\lambda$, $\sigma$, $k_{ef}^2 = \frac{e_0^2}{\varepsilon c} \ll 1$ and $\sigma_m = \omega_m \varepsilon \varepsilon_0$ denote a SAW wavelength, ZnO film sheet conductivity, effective electro-mechanical coupling coefficient and the material constant, respectively. Thus, when the sheet conductivity of the ZnO

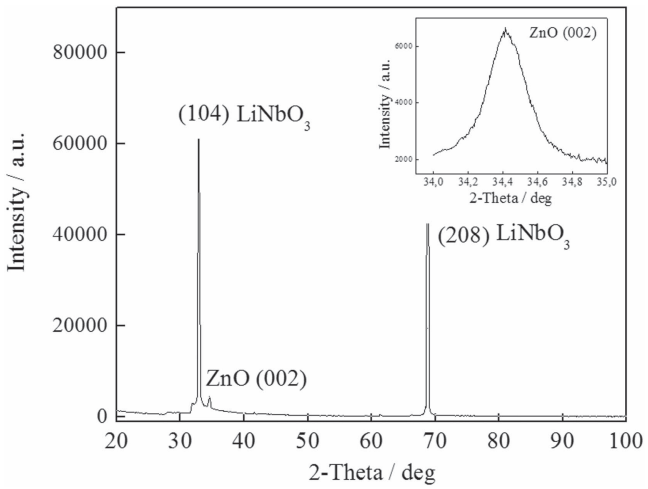


**Figure 2.** XRD spectrum of a typical ZnO/$LiNbO_3$ film. The ZnO (002) peak is shown in the inset.

film is limited to $\sigma_m$ value, the attenuation $\Gamma$ of a SAW reaches a maximum. The initial sheet resistance of the ZnO layer for Sample A grown at 500 °C was as high as $\sim 6.75 \times 10^3$ Ohm · cm and is several times higher than the one for Sample B ($1.375 \times 10^3$ Ohm · cm) for which the temperature was increased to 550 °C. Under illumination by UV light of a HeCd laser at 325 nm with intensity of 3.2 mW $cm^{-2}$ the sheet resistance decreased to $\sim 6.52 \times 10^3$ and $\sim 1.1 \times 10^3$ Ohm · cm for Sample A and B, respectively. The frequency response ($S_{21}$) of the ZnO/ $LiNbO_3$ SAW photo-detector (Sample A) is shown in figure 3(a). Once a SAW starts propagating, the response reveals an interference picture. The distance between neighboring maxima is equal to ~70 kHz, which corresponds to a time delay of ~14.3 $\mu$s, which is the time needed for a SAW with a velocity of 3980 m $s^{-1}$ to propagate the distance of ~5.7 cm between IDTs. The SAW detector-time response, which is a Fourier transform of the $S_{21}$ characteristic is shown in figure 3(b). When a SAW is reflected from the IDTs, second, third and higher-order reflections are observed at 28.4, 42.6 $\mu$s, etc. The absence of the additional reflections due to intersections of pieces was guaranteed by the absence of extra peaks in the Fourier transform of the frequency response. The attenuation of a SAW propagating in Sample A with a low conductivity of the ZnO layer is very low and, thus, up to seven SAW reflections are detected, as shown in figure 3(b). More specifically, a 'native' SAW attenuation induced by the ZnO layer in the dark can be roughly estimated from the first to second peak intensity ratio. Note that a SAW attenuation caused by reflection from the IDT also contributes to this value. In particular, in Sample A the SAW is attenuated for 9.4 dB, because of the acousto-electronic effect caused by carriers present in the ZnO film and a reflection from the IDT. Even at the highest applied incident UV-light intensity, the photo-detector does not show complete attenuation of the $S_{21}$ characteristics, as shown in figure 3(a). Two opposite cases of peak attenuation, corresponding to the high/low incident UV-light intensity of 280 and 2.8 mW $cm^{-2}$ are illustrated in

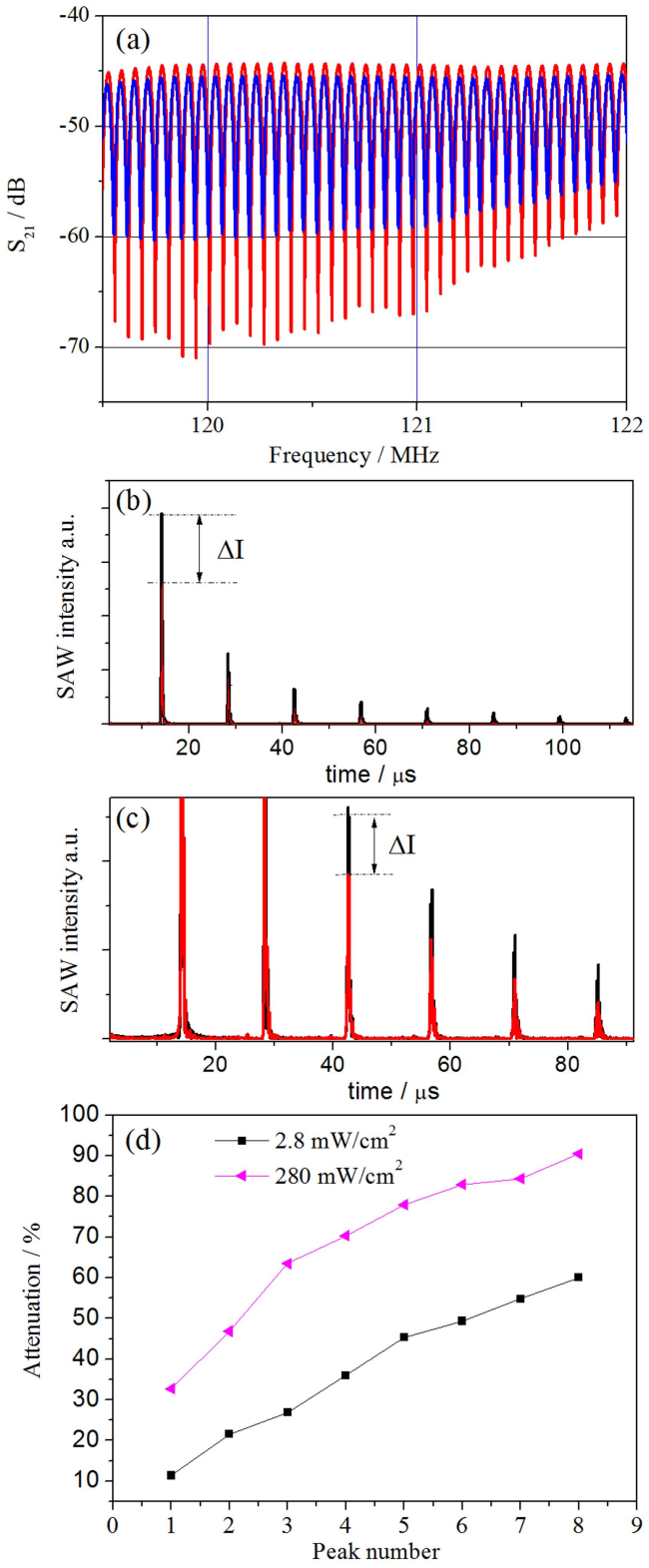


**Figure 3.** Frequency response ($S_{21}$) of the ZnO/$LiNbO_3$ SAW detector (Sample A) in dark (red) and under illumination by UV light at 325 nm and intensity of 280 mW $cm^{-2}$ (blue) (a); Fourier transform of $S_{21}$ characteristics with (red)/without (black) UV light at intensity of 280 mW $cm^{-2}$ (b) and 2.8 mW $cm^{-2}$ (c); attenuation of peaks in time response characteristics of the SAW detector (d).

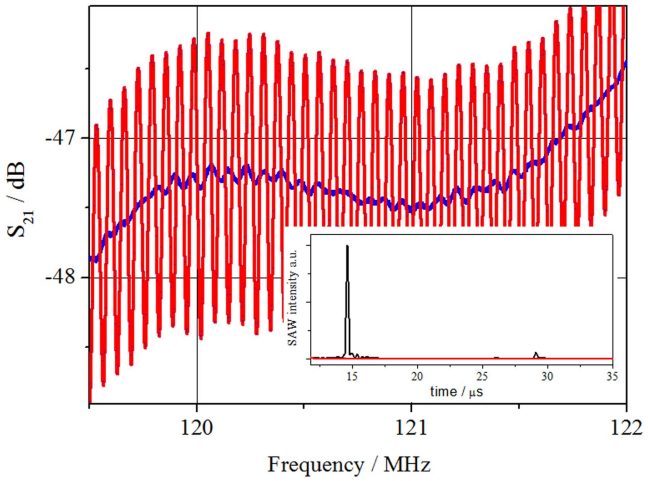


**Figure 4.** Frequency response ($S_{21}$) of Sample B in the dark (red) and under illumination by UV light at 325 nm and 280 mW cm$^{-2}$ (blue) and corresponding Fourier transform of $S_{21}$ characteristics with (red)/without (black) UV light.

figures 3(b) and (c). Attenuation of the peaks, corresponding to the SAW propagating through the Sample A several times, is presented in figure 3(d). When the light intensity is as high as 280 mW cm$^{-2}$ the first peak of the $S_{21}$ Fourier transform characteristics is attenuated by ~30% and, thus, may be used to measure the UV-light power, as shown in figure 3(b). For low incident intensity of 2.8 mW cm$^{-2}$ the first peak at 14.3 $\mu$s does not change much and it cannot be used for light detection any more. However, the attenuation of higher-order SAW reflections is feasible to monitor the light intensity. In particular, the attenuation of ~27% and ~60% for the 2nd and 7th SAW reflections were detected, respectively, as illustrated in figure 3(d). The UV-light-induced SAW delays did not exceed ~0.02–0.04 $\mu$s even at the highest used light power and, thus, they cannot be seen in figures 3, 4 and may hardly be used for reliable light detection.

The ZnO film of Sample B with higher conductivity shows only ~2–3 SAW reflections from the IDTs, which evidences that a propagating SAW is considerably attenuated even in the dark. From the first to second peak intensity ratio, one can find that the SAW attenuation in the ZnO film induced by acousto-electric effect in the dark is already as high as 28,1 dB. The sheet conductivity of the ZnO layer for Sample B is much higher than the one for Sample A and, according to equation (1), is much closer to $\sigma_m$ value even in the dark. When the detector is exposed to UV light, the film conductivity is further increased and is limited to $\sigma_m$ value, which is accompanied by additional SAW attenuation. In contrast to Sample A, the frequency response ($S_{21}$) of Sample B shows complete saturation at UV-light intensity of 280 mW cm$^{-2}$, as shown in figure 4. As can be seen from the Fourier transform of the $S_{21}$ characteristic in the inset of figure 2, the SAW propagating in Sample B is nearly completely attenuated already after the first pass.

A typical photo-electric response of Sample A and B at moderate intensity of 3.2 mW cm$^{-2}$ is shown in figure 5. Sample A shows fast response and conductivity recovery

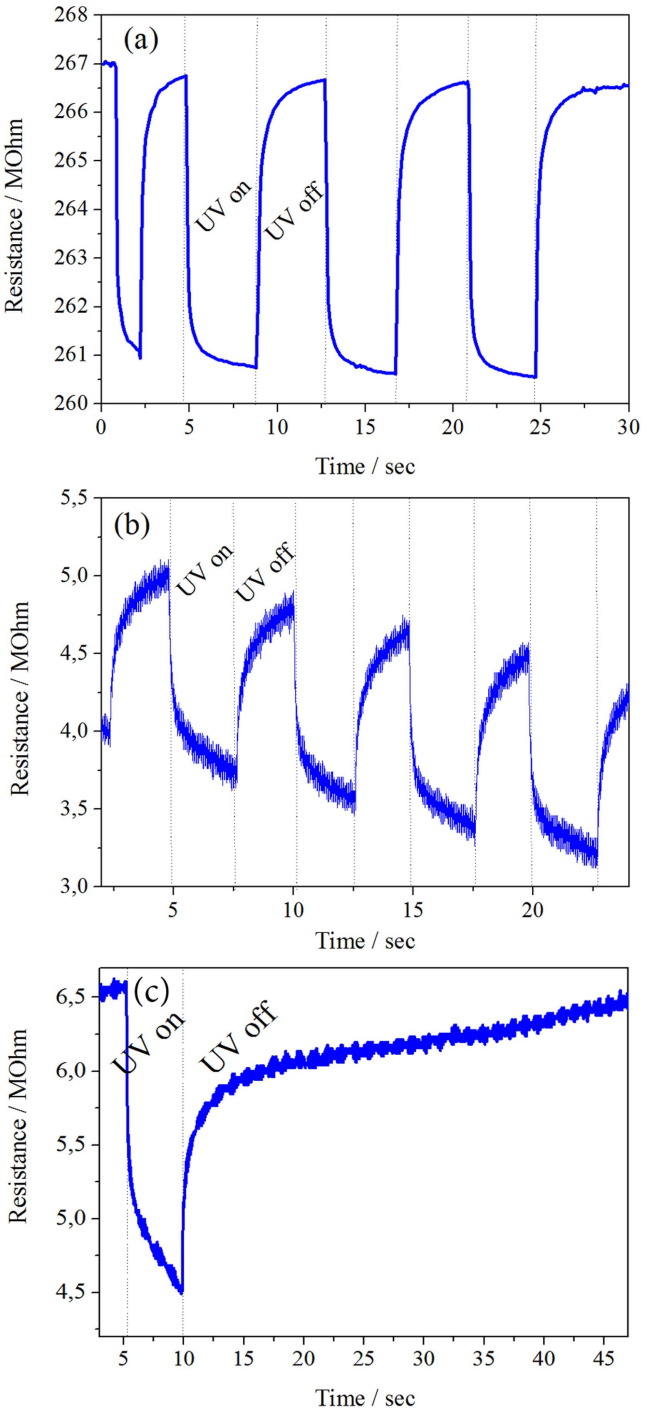


**Figure 5.** ZnO resistance change in Sample A (a) and B (b), (c), measured with/without illumination by UV light 325 nm (HeCd laser) and intensity of 3.2 mW cm$^{-2}$.

time, as presented in figure 5(a), whereas the resistance of Sample B drops and recovers very slowly (~40 s), as shown in figures 5(b), (c). Note that the photo-response kinetics shown in figure 3 was measured using a mechanical chopper and presented here as a qualitative illustration of the difference in response of the two detectors. The time-resolved photo-response of the 'fast' photo-detector A is characterized more accurately below. The long recovery time of the ZnO film for Sample B is similar to those reported previously

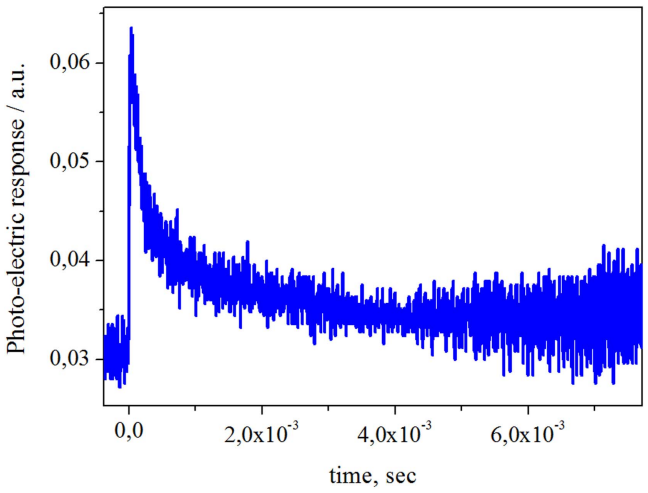


**Figure 6.** Time-resolved photo-electric response of ZnO film in Sample A, measured under illumination by 15 nm pulse of the third harmonic of the YAG:$Nd^{+3}$ laser at 355 nm with fluence of 23 mJ $cm^{-2}$.

[7, 8, 10, 12–14] and is likely caused by oxygen-related long-living trap states inside of the semiconductor band gap.

To accurately characterize the photo-electric response kinetics of the ZnO film for Sample B, we measured a resistance change kinetics under excitation by 15 ns laser pulse of the third harmonics of the YAG:Nd laser.

The measured photo-response shown in figure 6 was fitted with a double exponential function as:

$$I = A_1 \exp\left(-\frac{t}{\tau_{\text{slow}}}\right) + A_2 \exp\left(-\frac{t}{\tau_{\text{fast}}}\right)$$

The corresponding fast and slow components of the kinetics were found to be $\tau_{\text{fast}} = 0.14 \pm 0.08$ ms and $\tau_{\text{slow}} = 1.3 \pm 0.01$ ms. The recovery time is several orders of magnitude shorter than those for other UV SAW photo-detectors previously presented, where recovery times as long as 2.4–30 s were reported [7, 8, 10, 12–14]. The time, which the SAW with velocity of 3980 m $s^{-1}$ spends to propagate 1 cm under the ZnO film is ~2.5 us. As the photo-response relaxation time is more than ~160 times longer than the time during which the SAW propagates in the ZnO layer, one may consider that the process is stationary, i.e. the ZnO sheet conductivity does not change during the acousto-electronic interaction of carriers with the wave. The relaxation time of the SAW photo-detector with the ZnO film, similar to that of Sample A, is limited by the slowest process, i.e. by the relaxation time of the photo-generated carriers. As shown above, the ZnO film in Sample A (with higher sheet resistance) shows fast photo-electric response, but lower UV-light induced change in resistance. Therefore, a relative change in the intensity in the fundamental peak of the $S_{21}$ Fourier transform is lower than the one for Sample B. If using a fundamental peak change for photo-detection, one could consider that the ZnO film similar to the one in Sample B is more advantageous. However, the high sensitivity of the ZnO film in Sample B towards UV light is accompanied by very slow response. To overcome this 'slow response' limitation, one may design a photo-detector with a ZnO layer of the Sample A type and use one of the SAW reflections for detection as a better alternative. In this way, a SAW propagates several times back and forth and the resulting effect of the SAW interaction with light is larger. Thus, the drawbacks related to low sensitivity of ZnO film can be easily compensated by using our approach to monitor multiple SAW reflections of a photo-detector device.

## 4. Conclusions

In summary, we presented a new approach to enhance the sensitivity of the existing SAW UV-visible photo-detectors by using multiple reflections of the acoustic waves. We show that the ultrafast SAW UV photo-detector with millisecond response may be obtained by tuning the deposition conditions of the ZnO film. Applying the concept of monitoring the intensity of the multiple SAW reflections in Fourier transform of the frequency response ($S_{21}$) an ultrahigh sensitivity of a SAW photo-detector may be achieved. To detect high incident light intensity, one may monitor only the fundamental peak of a time response.

## Acknowledgments

The work was supported by the Ministry of Education and Science of the Russian Federation, project No. 16.219.214/K 'Development of ZnO nanowire-based systems synthesis methods for photo-detectors, optical nanoantennas and piezo- and chemisensors elements'.

## References

[1] Marcu A and Viespe C 2015 Laser-grown ZnO nanowires for room-temperature SAW-sensor applications *Sensors Actuators* B **208** 2
[2] Sharma P and Sreenivas K 2003 Highly sensitive ultraviolet detector based on ZnO/$LiNbO_3$ hybrid surface acoustic wave filter *Appl. Phys. Lett.* **83** 3617
[3] Tsai W C, Kao H L, Liao K H, Liu Y H, Lin T P and Jeng E S 2015 Room temperature fabrication of ZnO/ST-cut quartz SAW UV photodetector with small temperature coefficient *Opt. Express* **23** 2187
[4] Kumar S, Kim G H, Sreenivas K and Tandon R P 2009 ZnO based surface acoustic wave ultraviolet photo sensor *J. Electroceram.* **22** 198
[5] Emanetoglu N W, Zhu J, Chen Y, Zhong J, Chen Y and Lu Y 2004 Surface acoustic wave ultraviolet photodetectors using epitaxial ZnO multilayers grown on r -plane sapphire *Appl. Phys. Lett.* **85** 3702
[6] Wei C L, Chen Y C, Cheng C C, Kao K S, Cheng D L and Cheng P S 2010 Highly sensitive ultraviolet detector using a ZnO/Si layered SAW oscillator *Thin Solid Films* **518** 3059
[7] Peng W, He Y, Wen C and Ma K 2012 Surface acoustic wave ultraviolet detector based on zinc oxide nanowire sensing layer *Sensors Actuators* A **184** 34

[8] Chivukula V, Ciplys D, Shur M and Dutta P 2010 ZnO nanoparticle surface acoustic wave UV sensor *Appl. Phys. Lett.* **96** 233512

[9] Jo M, Lee K J and Yang S S 2014 Sensitivity improvement of the surface acoustic wave ultraviolet sensor based on zinc oxide nanoparticle layer with an ultrathin gold layer *Sensors Actuators* A **210** 59

[10] Peng W, He Y, Xu Y, Jin S, Ma K, Zhao X, Kang X and Wen C 2013 Performance improvement of ZnO nanowire based surface acoustic wave ultraviolet detector via poly (3,4-ethylenedioxythiophene) surface coating *Sensors Actuators* A **199** 149

[11] Kumar S, Sharma P and Sreenivas K 2005 Low-intensity ultraviolet light detector using a surface acoustic wave oscillator based on $ZnO/LiNbO_3$ bilayer structure *Semicond. Sci. Technol.* **20** L27

[12] He X L, Zhou J, Wang W B, Xuan W P, Yang X, Jin H and Luo J K 2014 High performance dual-wave mode flexible surface acoustic wave resonators for UV light sensing *J. Micromech. Microeng.* **24** 055014

[13] Pang H F, Fu Y Q, Li Z J, Li Y F, Ma J Y, Placido F, Walton A J and Zu X T 2013 Love mode surface acoustic wave ultraviolet sensor using ZnO films deposited on 36°Y-cut $LiTaO_3$ *Sensors Actuators* A **193** 87

[14] Wang W, Gu H, He X, Xuan W, Chen J, Wang X and Luo J K 2014 Thermal annealing effect on ZnO surface acoustic wave-based ultraviolet light sensors on glass substrates *Appl. Phys. Lett.* **104** 212107

[15] Kaidashev E M, Lorenz M, Wenckstern H, von, Rahm A, Semmelback H C, Han K H, Bendorf G, Bundesmann C, Hochmuth H and Grundmann M 2003 High electron mobility of epitaxial ZnO thin films on c-plane sapphire grown by multistep pulsed-laser deposition *Appl. Phys. Lett.* **82** 3901

[16] Rotter M, Wixforth A, Ruile W, Bernklau D and Riechert H 1998 Giant acoustoelectric effect in $GaAs/LiNbO_3$ hybrids *Appl. Phys. Lett.* **73** 2128